Int J Thermophys (2017) 38:129
DOI 10.1007/s10765-017-2264-0

ICPPP 18

Study of the Solidification Dynamic of a Photocurable Resin by Photoacoustic

J. L. Jiménez-Pérez[1] · A. Cruz-Orea[2] · P. Vieyra Pincel[1] · Z. N. Correa-Pacheco[3]

Received: 14 November 2013 / Accepted: 20 June 2017 / Published online: 4 July 2017

Abstract This paper reports on the photoacoustic (PA) study of a photopolymer (resin) that changes its physical properties when being irradiated with ultraviolet light from a xenon lamp. The wavelength range necessary for the curing of the resin, characterized by the PA technique, was found to be between 300 nm and 400 nm. PA measurements show a sigmoidal change of heat transport properties as a function of time during the curing process. By describing the PA signal evolution by a parametrized model, a characteristic curing time was introduced. The PA measurements were complemented with UV–Vis Spectroscopy, which was used to characterize the polymer in order to study the optical absorption. The proposed method can support the optimization of the settings of curing parameters in applications of stereolithography and 3D printing.

Keywords 3D · Curing · Photoacoustic · Resin · Stereolithography · UV

This article is part of the selected papers presented at the 18th International Conference on Photoacoustic and Photothermal Phenomena.

✉ J. L. Jiménez-Pérez
jimenezp@fis.cinvestav.mx

1 UPIITA-Instituto Politécnico Nacional, Avenida Instituto Politécnico Nacional, No. 2580, Col. Barrio la Laguna Ticomán, Delegación Gustavo A. Madero, C.P. 07340 Ciudad de México, Mexico

2 Departamento de Física, CINVESTAV-IPN, Av. Instituto Politécnico Nacional 2508, Col. San Pedro Zacatenco, C.P. 07360 Ciudad de México, Mexico

3 CEPROBI-Instituto Politécnico Nacional, Carretera Yautepec-Jojutla, Km. 6, calle CEPROBI No. 8, Col. San Isidro, Yautepec, Apartado Postal 24, C.P. 62731 Morelos, Mexico

1 Introduction

3D printing is a process of making a three-dimensional solid object of virtually any shape from a digital model. This is achieved by adding successive layers of material (liquid resins) in different shapes. 3D printing technology is used for both prototyping and distributed manufacturing with applications in industrial design, automotive, aerospace, engineering, dental and medical, and many other fields [1–8]. Our principal objective in this work is the study and characterization of a resin that is used in 3D printing. A photoacoustic (PA) technique is used to monitor the structural changes that go along with the UV illumination-induced curing process and to estimate the characteristic curing time.

2 Experimental Apparatus and Procedures

The curing of an acrylic resin sample (Intek, Mexico) was monitored while it was lying on an aluminum foil that closed the top side of a photoacoustic cell. The sample layer was illuminated from the top side by mechanically chopped UV light, 388 nm wavelength, by use of a monochromator in order to choose this wavelength from a Xe lamp. The light power was 0.16 mW, and the spot size had 2 mm diameter. Due to optical absorption, the periodical illumination produced a periodical thermal wave that diffused through the sample and aluminum layer into the PA cell. The resulting periodical thermal expansion of an air layer adjacent to the bottom of the aluminum foil gave rise to a periodical pressure oscillation in the cell (volume 85 mm^3), which was detected by a Radio Shack electret microphone. The pressure oscillation temperature was determined by means of a dual phase lock-in amplifier. A modulation frequency of 17 Hz gave the largest signal. The experimental setup is shown in Fig. 1.

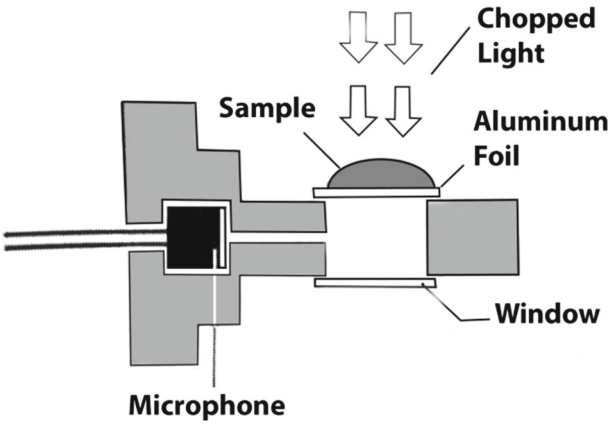

Fig. 1 Diagram of the photoacoustic cell used in this study

3 Theory

The pressure oscillation in the PA cell is proportional to the temperature oscillation at the aluminum–air interface, as given by the following expression, which was determined by Rosencwaig and Gersho [9]:

$$S \cong \frac{(1-i)}{2a_g}\left(\frac{\sqrt{2}}{\sqrt{\omega}}\frac{1}{e_b}\right) Y(f)\,\mathrm{Taa}(f) \tag{1}$$

where $i = \sqrt{-1}$, a_g is the thermal diffusion coefficient of the air inside the PA chamber being $a_g = (1+i)/\mu_g$, μ_g the thermal diffusion length in air, given by $(\alpha_g/(\pi f))^{1/2}$, e_b the effusivity of aluminum, f the chopping frequency of the incident light beam, $\omega = 2\pi f$ the angular frequency, Taa(f) the temperature oscillation at the aluminum–air interface, $Y(f)$ an instrumental factor that depends on the microphone and on the acoustic response of the PA cell. This enables the PA technique to indirectly monitor different processes that change the structure and consequently the thermal properties of materials in the base position.

Since at the used frequency of 17 Hz, the thermal diffusion length in aluminum (45 μm, at 17 Hz) is much larger than the foil thickness (16 μm), the surface temperature oscillation at the aluminum–air interface is roughly equal to the one at the sample–aluminum interface, Tsa(f). Since the sample is semitransparent for the PA signal generating modulated UV radiation, Tsa(f) depends in a rather complicated way on the thermal and optical properties of the sample. Simplification of the model is only possible if the UV penetration depth is either much shorter or much longer than the sample thickness. The model proposed in Eq. 1 assumes that all the heat is produced at the sample–aluminum interface, most likely not be suitable. If the model is used anyway, then the value of the UV absorption coefficient and penetration depth should be given and it should be much larger than the sample thickness. If the UV penetration depth is of the order of the sample thickness or shorter, then the model should be refined with a finite optical absorption coefficient in an air–sample–(aluminum)–air configuration with a heat source $I = I_o \exp(-\beta_{\mathrm{UV}} x)$, with x the depth coordinate that is zero at the air–sample interface.

4 Results and Discussion

The optical absorption spectrum of the liquid resin was obtained by using UV–Vis spectrophotometry. Figure 2 shows in the spectrum, an optical absorption band of the resin from 340 nm to 405 nm. We have chosen a 388 nm wavelength in order to analyze the curing process of the photosensible resin since for this wavelength the sample is optically opaque. In that case, the Rosencwaig and Gersho model for an optically opaque sample can be used [9].

The time evolution of the PA signal in Fig. 3 (red line) shows a saturating exponential decay with curing time for the sigmoidal model, which we have fitted by the following expression:

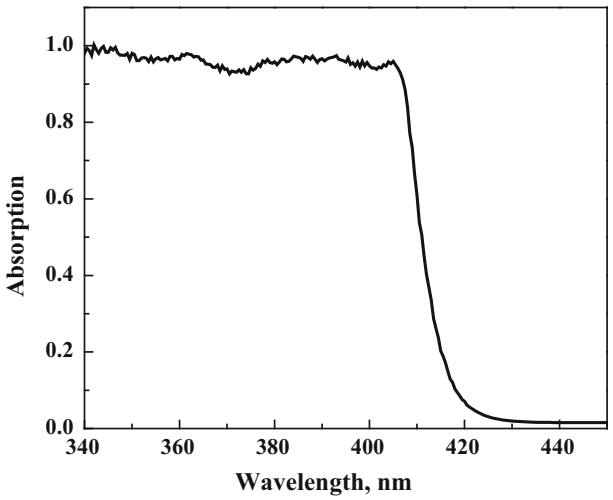

Fig. 2 Absorption spectrum of resin

$$S(t) = A_1 + A_2{}^*(\mathrm{e}^{-(t-t_0)/\tau}) \tag{2}$$

with A_1 the saturation level, A_2 the difference between the initial and final level, t_0 the initial time, and τ representative for the time needed for the PA signal to reach a final steady-state level, which in turn is related to the curing time. Fitting Eq. 2 to the experimental data, values for the parameter t_0, the start of UV illumination and $\tau = 52.41$ min were found, for a resin thickness of 711 μm. In order to measure the liquid resin thickness, there were used several commercial steel plates with very well-known thicknesses, also the resins thicknesses was corroborated with a Vernier. Figure 3 shows for a sample of 711 μm thickness that the fitted PA signal is increasing and then saturates. This observation infers that the PA signal is probing the evolution of the solid–liquid resin interface, which moves with time from the top of the resin toward the aluminum foil. The PA signal is sensitive to the resin region next to the aluminum foil reaching till about one thermal diffusion length of resin into the resin. At the used modulation frequency of 17 Hz, the thermal diffusion length is about 45 μm. Before the start of the curing, the PA signal reflects the thermal effusivity of the liquid resin. As the curing is progressing, the resin solidification front is entering the zone near the aluminum foil, so that the probed effusivity is evolving to the value of the cured resin. The increasing PA signal amplitude reflects that the solid resin has a lower effusivity than the liquid one. The PA signal increase saturates once the sample is fully cured. The thinner the sample, the faster full curing is established.

The curing experiment was repeated on fresh resin samples of six thicknesses ($l = 203$ μm, 305 μm, 406 μm, 508 μm, 610 μm and 711 μm). As the resin is rather thin, we have implemented the theoretical model assuming that the UV-induced heat distribution is uniform. This is valid for the first two samples (thickness $l = 203$ and 305), since the optical depth (the inverse of the optical absorption coefficient) is 350 μm and the thickness of the first two samples is smaller than 350 μm.

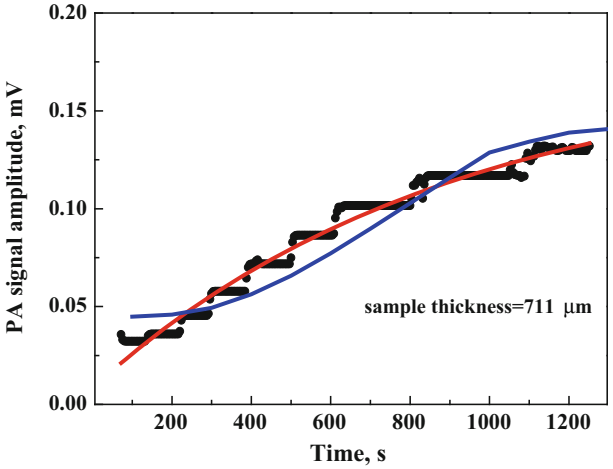

Fig. 3 Evolution of the experimental PA signal (*black symbols*) and the theoretical simulation from two-layer model (*red line*) and three-layer model (*blue line*) as a function of time for resin (Color figure online)

Figure 4 shows the dependence of the fitted PA saturation time on the sample thickness. The extracted saturation time increases with increasing sample thickness, suggesting the following scenario. The curing occurs and finalizes faster in shallow parts of the sample and affects increasingly deeper regions as time evolves. The PA signal thus probes a varying combination of more fully cured material near the upper boundary and less cured material near the lower boundary of the sample. The thicker the sample, the longer it takes until the front between already fully cured and not fully cured reaches the lower boundary of the sample. The reason for the curing starting earlier in the upper region of the sample can be that, although curing immediately starts throughout the sample, because of the finite UV penetration depth, more shallow parts of the sample experience a higher UV intensity and thus a shorter curing time than deeper parts. The thicker the sample, the lower the UV intensity in the deepest parts of the sample, and the longer the curing time. For thin samples, the curing time saturates at about 700 s for the used UV intensity. The data in Fig. 3 are step-like because the resin curing is developed in a growing process layer by layer.

A similar scenario for the curing process, involving an effective thermal diffusion length, which depends on the amount of liquid and cured resin was proposed in reference [10]. In this reference, the authors define an effective thermal diffusion length which depends on both materials (liquid resin and cured resin). The cure of the resin begins on the top (surface in contact with air) and finishes in the surface in contact with the reference material (aluminum). The cured/liquid resin assembly can be considered as a homogeneous two-layer system that changes in thickness and in thermal properties as a function of time [11].

Also by making a new theoretical analysis, it is possible to obtain the experimental PA signal of the cured resin as a function of time (Fig. 3, blue line). In Fig. 3, we show experimental PA signal as function of time (black symbols) and the simulation from Eq. 1 for sample with total thickness of 711 μm.

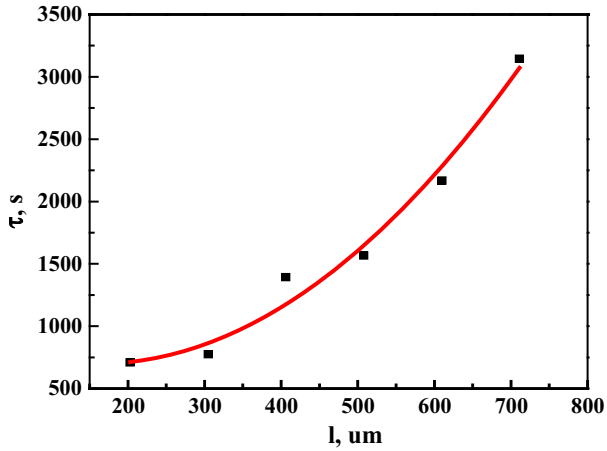

Fig. 4 Variation of the cured thickness as a function of the characteristic time of curing for $\lambda = 388\,\text{nm}$

In order to model the photothermal temperature variation (proportional to the photoacoustic signal) at the detection (back) side of the two-layer model, we have made use of the fact that the UV penetration depth (350 μm) is larger than the thickness of majority of samples, so that the UV heat distribution generating the photothermal signal can be considered to be spatially uniform. A four-layer system was considered: air cavity, liquid resin, solid resin, air above sample.

By using the model, the ratio between the initial and final signal magnitude can be predicted, which was found to be directly connected with the effusivity ratio between the liquid and solid samples. This model is applicable because the UV light is penetrating the sample ($\beta = 28.21\,\text{cm}^{-1}$ and optical depth is $\mu_\beta = 0.35\,\text{mm}$), which means that we have a uniform heating model of a three-layer system: air cavity, liquid resin, solid resin, air above sample. This model can make use of the ratio of the initial and final signals, which reflects the effusivity ratio between liquid and solid samples. In order to make simulations, an estimate should be determined for the thermal diffusivity of the liquid resin. The model also requires the value of the UV absorption coefficient in cured and liquid resins.

The model infers that, if the assumptions made are valid, the ratio of signal amplitudes of the totally cured and totally liquid sample (Fig. 3), $S(\text{total cured})/S(\text{total liquid}) = 0.131/0.033 = 4$, corresponds with the ratio of the effusivity of the solid and liquid resins. The ratio probably reflects the ratio of the effusivities of solid and liquid resins as long as the UV penetration depth is not known, no conclusions can be drawn.

5 Conclusions

The time evolution of the curing process of resin was monitored by the photoacoustic technique, in which the temperature variation at the interface between the sample–aluminum foil interfaces adjacent to the PA microphone cell is detected. The time

evolution of the PA signal was interpreted in the framework of a scenario in which with increasing curing time, the average thermal diffusivity and effusivity in the sample, both of which affect the PA signal magnitude, evolve from the value of liquid to the one of solid resin. The detection principle exploits the difference in thermal effusivity between the cured and liquid resins. As the sample is curing from the illuminated side toward the bottom of the sample, the cured part of the sample enters the probed region of the sample, within a thermal diffusion length from the aluminum foil. In this way, the PA signal evolves from a value determined by the liquid resin's effusivity toward a value determined by the effusivity of the cured resin, with a characteristic time that reflects the curing time of the sample. This model was confirmed by the decrease in the characteristic time of the PA signal with decreasing resin layer thickness.

The results demonstrate that PA microphone cell detection can be adequately used to monitor the resin curing process. The behavior of the PA signal, as a function of time, shows a saturating growth during the curing process. The time evolution of the PA signal is characterized by a saturation that goes along with a fully cured resin layer. The parameterization of these curves permitted the determination of the characteristic curing time of the process. Also a theoretical analysis for the two-layer samples (cured and liquid resins) was developed to obtain the dynamic of the experimental PA signal when the sample goes from totally liquid to totally cured. The theoretical evolution of the experimental PA signal fits very well with the experimental data. These results provide an alternative technique for quantitative control in curing monitoring and measurements of optimal times in manufacturing processes for applications in stereolithography and 3D printing.

Acknowledgements We would like to thank CONACYT, COFAA and CGPI-IPN, México. One of authors (A. Cruz-Orea) thanks the partial support for this research from Conacyt Project No. 241330.

References

1. M.S. Mannoor, Z. Jiang, T. James, Y.L. Kong, K.A. Malatesta, W.O. Soboyejo, N. Verma, D.H. Gracias, Ml C. McAlpine, NanoLetters **13**(6), 2634 (2013)
2. C. Stapleton, Inside Dent. Technol. **4**(4), 01 (2013)
3. P.N. Patel, C.K. Smith, C.W. Patrick, J. Biomed. Mater. Res. A **73**(3), 313–931 (2005)
4. David H. Freedman, Layer by layer. Technol. Rev. **115**(1), 50 (2012)
5. F.L. Dumas, F.R. Marciano, L.V.F. Oliveira, P.R. Barja, D. Acosta Avalos, Med. Eng. Phys. **29**, 980 (2007)
6. P. Martinez Torres, A. Mandelis, J.J. Alvarado Gil, J. Appl. Phys. **108**, 054902 (2010)
7. A. Christ, J. Szurkowski, Instrum. Sci. Technol. **29**(2), 91 (2001)
8. G. Bogoeva-Gaceva, A. Bužarovska, Maced. J. Chem. Chem. Eng. **32**(2), 337 (2013)
9. A. Rosencwaig, A. Gersho, J. Appl. Phys. **47**, 64 (1976)
10. M. Vargas-Luna, G. Gutierrez, J.M. Rodriguez Viscaino, J.B. Varela Najera, J.M. Rodriguez Palencia, J. Bernal-Alvarado, M. Sousa, J.J. Alvarado-Gil, J. Phys. D Appl. Phys. **35**, 1532 (2002)
11. A.M. Manzanares, A.C. Bento, H. Vargas, N.F. Leite, L.C.M. Miranda, Phys. Rev. B **42**, 4477 (1991)